Published in final edited form as:
Cancer Res. 2012 October 1; 72(19): 4984–4992. doi:10.1158/0008-5472.CAN-12-1831.

Cardiac inflammation after local irradiation is influenced by the kallikrein-kinin system

Vijayalakshmi Sridharan[1], **Preeti Tripathi**[1], **Sunil K. Sharma**[2], **Eduardo G. Moros**[3], **Peter M. Corry**[2], **Benjamin J. Lieblong**[4], **Elena Kaschina**[5], **Thomas Unger**[5], **Christa Thöne-Reineke**[5], **Martin Hauer-Jensen**[1,6], and **Marjan Boerma, PhD**[1]

[1]University of Arkansas for Medical Sciences, Department of Pharmaceutical Sciences, Division of Radiation Health, Little Rock, Arkansas

[2]University of Arkansas for Medical Sciences, Department of Radiation Oncology, Little Rock, Arkansas

[3]Moffitt Cancer Center and Research Institute, Department of Radiation Oncology, Tampa, Florida

[4]University of Arkansas for Medical Sciences, Department of Pharmacology and Toxicology, Little Rock, Arkansas

[5]Charité University, Institute of Pharmacology, Berlin, Germany

[6]Surgical Service, Central Arkansas Veterans Healthcare System, Little Rock, Arkansas

Abstract

Radiotherapy of intrathoracic and chest wall tumors may lead to exposure of the heart to ionizing radiation, resulting in radiation-induced heart diseases (RIHD). The main manifestations of RIHD become apparent many years after treatment and include cardiomyopathy and accelerated atherosclerosis. This study examines the role of the kallikrein-kinin system (KKS) in RIHD by investigating the cardiac radiation response in a kininogen-deficient Brown Norway Katholiek (BN/Ka) rat model. BN/Ka rats and wild-type Brown Norway (BN) rats were exposed to local heart irradiation with a single dose of 18 Gy or 24 Gy and were observed for 3-6 months. Examinations included *in vivo* and *ex vivo* cardiac function, histopathology, gene and protein expression measurements, and mitochondrial swelling assays. Upon local heart irradiation, changes in *in vivo* cardiac function were significantly less in BN/Ka rats. For instance, a single dose of 24 Gy caused a 35% increase in fractional shortening in BN rats compared to a 16% increase in BN/Ka rats. BN rats, but not BN/Ka rats, showed a 56% reduction in cardiac numbers of CD2-positive cells, and a 57% increase in CD68-positive cells, together with a 52% increase in phosphorylation of Erk1/2. Local heart irradiation had similar effects on histopathology, mitochondrial changes, and left ventricular mRNA levels of NADPH oxidases in the two genotypes. These results suggest that the KKS plays a role in the effects of radiation on cardiac function and recruitment of inflammatory cells. The KKS may have these effects at least in part by altering Erk1/2 signaling.

Correspondence: Marjan Boerma, PhD University of Arkansas for Medical Sciences Department of Pharmaceutical Sciences, Division of Radiation Health 4301 West Markham, Slot 522-10 Little Rock, AR 72205 Phone: 501-686-6599 Fax: 501-686-6057 mboerma@uams.edu.

Conflicts of interest: None

Keywords

Radiation-induced heart disease; Kallikrein-kinin system; Bradykinin

Introduction

Radiation-induced heart diseases (RIHD) are a long-term side effect of radiotherapy of intrathoracic and chest wall tumors when radiation fields encompass all or part of the heart, such as, in Hodgkin's disease (1) or breast cancer (2). Manifestations of RIHD include accelerated atherosclerosis, pericardial and myocardial fibrosis, conduction abnormalities, and injury to cardiac valves (3). Both incidence and severity of the disease increase with higher radiation dose-volume, younger age at time of exposure, and greater time elapsed since treatment. The only available approach to reduce late complications in the heart is through efforts to reduce cardiac radiation dose during therapy. Indeed, radiotherapy has undergone many such improvements over the last decades. Nonetheless, recent studies indicate that some patients with Hodgkin's disease, lung cancer, esophageal and proximal gastric cancer still receive either a high dose of radiation to a small part of the heart or a lower dose to the whole heart (4-6). Biological mechanisms of RIHD are largely unknown, and research is required to unravel the underlying mechanisms in an effort to identify potential targets for intervention.

Bradykinin and kallidin are peptide hormones involved in platelet aggregation, angiogenesis, inflammation, and acute phase response that are formed in the kallikreinkinin system (KKS) by proteolytic cleavage of both high-molecular weight kininogen (HK) and low-molecular weight kininogen (LK). The production of kinins occurs by kallikrein enzymes in plasma and tissues, and by mast cell-derived proteases (7, 8). The two best known kinins are bradykinin and kallidin, which affect their target cells via two receptors, B1 and B2. While the B2 receptor is constitutively expressed in the heart, the B1 receptor is expressed only under certain circumstances of inflammation or tissue injury (9). Both receptors may be upregulated in the heart under ischemia, inflammation, and adverse remodeling (10). Some of the intracellular signaling pathways induced by kinin receptor activation involve Akt and Erk1/2 (11, 12). Kinin signaling is sometimes considered to aggravate cardiac disease with a significant inflammatory component, such as myocardial infarction (13). On the other hand, kinins are well known for their induction of nitric oxide and prostacyclin, mediating cardioprotection via vasodilation and inhibition of cardiac fibroblasts (14, 15).

Brown Norway Katholiek (BN/Ka) rats are deficient in HK and LK due to a point mutation in the kininogen gene (16). BN/Ka rats have been used to study the role of the KKS in several models of cardiovascular disease (17-19). This study examined the role of the KKS in RIHD by investigating molecular, structural, and functional changes after local heart irradiation in BN/Ka and wild-type Brown Norway (BN) rats. Both clinical and pre-clinical studies have shown that heart irradiation alters functional effects of irradiation in the lung (20, 21). In turn, the effects of pathological damage in the lung on function and structure of the heart have long been established. Because of known interactions between heart and lung, and potentially also the spinal cord, we used a new method of rat heart irradiation to limit radiation exposure of other tissues.

Materials and Methods

Kininogen-deficient animal model

BN rats were obtained from Harlan Laboratories (BN/RijHsd colony, Indianapolis, IN). BN/Ka breeder rats were a kind gift from Drs. Elena Kaschina and Thomas Unger (Charité University, Berlin, Germany). These rats carry a G to A point mutation at nucleotide 487 in the kininogen gene, resulting in an alanine to threonine exchange in both HK and LK. This amino acid exchange is responsible for the defective secretion of both kininogens from the liver (16, 22). As a result, BN/Ka plasma levels of HK, LK, and bradykinin are reduced 38-, 16.5- and 30-fold, respectively (18, 19). Because plasma kallikrein normally forms a complex with HK, plasma levels of kallikrein are also reduced in BN/Ka rats (23). Animals were housed 2-3 per cage in our Division of Laboratory Medicine on a 12:12 light-to-dark cycle with free access to food and water. All procedures in this study were approved by the Institutional Animal Care and Use Committee of the University of Arkansas for Medical Sciences.

Sequencing of kininogen

The sequence of the kininogen gene was assessed as described before (17). Total liver RNA was isolated with Ultraspec™ RNA reagent (Biotecx Laboratories, Houston, TX), treated with the Turbo DNA-free kit, and used for cDNA synthesis with the High Capacity cDNA Reverse Transcription kit (Applied Biosystems, Foster City, CA). The kininogen cDNA was amplified with the primers: 3'-ACGAGTACCACTGTCTGGG-5' and 3'-TGTTTGCACAATGGAGTAGA-5' in a touchdown PCR protocol: 95°C for 2 min, 30 cycles: 95°C for 30 s, 65°C (reduced by 0.5°C in each following cycle), 72°C for 40s, 10 cycles: 95°C for 30 s, 55°C for 30 s, 72°C for 40 s, final extension at 72°C for 3 min. PCR products were separated in a 2% agarose gel, extracted with a QIAquick Gel Extraction kit (Qiagen, Hilden, Germany), and sequenced in both directions with a 3100 Genetic Analyzer (Applied Biosystems). At least 6 rats of each experimental group were genotyped. All of the examined BN/Ka rats carried the G to A point mutation at the expected position, while all of the BN rats carried the wild-type genotype.

Local heart irradiation

Rats of 250-300 g were exposed to local heart irradiation with the Small Animal Conformal Radiation Therapy Device (SACRTD) developed at our institution. The SACRTD has a 225kVp X-ray source (GE Isovolt Titan 225) mounted on a custom made "gantry", a stage on a robotic-arm positioning system (Viper™ s650 Adept Technology, Pleasanton, CA), and a flat panel digital X-ray detector of 200 μm resolution (XRD 0820 CM3 Perkin Elmer, Fremont CA). For the purpose of local heart irradiation, a brass and aluminum collimating assembly produced a field of 19 mm diameter at the isocenter.

The dose rate at the isocenter was measured using a pin-point ion chamber (PTW N301013, ADCL calibrated for 225 kV) following the TG-61 protocol of the American Association of Physicists in Medicine. In addition, dosimetry was performed with Gafchromic® EBT-2 film (Ashland Specialty Ingredients, Wayne, NJ). A set of films was calibrated by exposing it to known doses on a Gamma Knife (Co-60) system, and the films were analyzed according to Devic et al. (24). A calibration curve was also drawn by exposing films with the SACRTD 225 kV X-ray beam. The films were energy independent and could be used for measurements of dose in the range used in our experiments. To measure relative depth dose, 11 pieces of film were placed in between 11 slabs of solid water phantom, each of 5 mm thickness. The top of the phantom was placed at the isocenter, perpendicular to the beam, and the films were exposed to 5 Gy at the isocenter (225 kV, 13 mA).

For local heart irradiation, rats were anesthetized with 3% isoflurane and placed horizontally in a Styrofoam holder. The X-ray source was tilted horizontally and a digital X-ray image was acquired with the detector (65 kV, 5 mA). The heart was localized and the gantry was tilted vertically for irradiation. The heart was irradiated at 225 kV, 13 mA, (0.5 mm Cu-filtration) resulting in 1.92 Gy/min at 1 cm tissue depth. The hearts were exposed in three 19 mm-diameter beams of 6 Gy or 8 Gy each. An angle of 30° between the beams (one vertical beam, one beam -30° from vertical, and one beam +30° from vertical) was established by tilting the platform.

Rats were observed for 3 months or 6 months after irradiation to determine cardiac function, structure, and molecular changes as described below.

Echocardiography

A Vevo 2100 high-resolution *in vivo* micro imaging system (VisualSonics, Toronto, Canada) with the MS250 MicroScan transducer (13-24 MHz) was used for echocardiography. Animals were anesthetized with 2% isoflurane and hair was removed from the chest with clippers and a depilatory cream. Short axis M-mode recordings at the mid left ventricular level were used to obtain echocardiographic parameters with the Vevo 2100 cardiac analysis software: thickness of the left ventricular anterior wall (LVAW), posterior wall (LVPW), inner diameter (LVID), volume, ejection fraction (EF), fractional shortening (FS), and stroke volume. B-mode recordings were used for strain analysis of three consecutive cardiac cycles using the Vevostrain™ software package (VisualSonics) (25). Recordings of the short axis were used to determine radial and circumferential velocity, displacement, peak strain and peak strain rate, and the long axis was used for longitudinal measurements.

Ex vivo-perfused rat heart preparations

Langendorff-type *ex vivo*-perfused rat heart studies were performed as described before (26). In short, rats were anesthetized with 3% isoflurane; hearts were isolated and immediately perfused via the aorta with an oxygenated Krebs-Henseleit solution (37°C) at a flow rate of 10 mL/g heart/min. The ventricles were paced with electrodes positioned on the interventricular septum to obtain a heart rate of 250 beats/min. Both atria were removed and a fluid-filled balloon connected to a pressure transducer (model PT300, Grass Technologies, West Warwick RI) was placed in the left ventricle to measure pressures at balloon volumes between 80 μL and 300 μL. Coronary pressure was monitored continuously with a second pressure transducer.

After Langendorff studies the hearts were weighed and processed for histology and immunohistochemistry.

Histology and immunohistochemistry

Hearts were fixed in methanol Carnoy's solution (60% methanol, 30% chloroform, 10% acetic acid) and embedded in paraffin. For both histology and immunohistochemistry, 5 μm sections were deparaffinized and rehydrated.

For determination of collagen, sections were incubated in Picrosirius red (American MasterTech, Lodi, CA) with Fast Green (0.01% w/v, Fisher Scientific, Pittsburgh, PA) for 2 hours. Sections were analyzed with an Axioskop transmitted light microscope (Carl Zeiss, Thornwood, NY) with a chilled color camera (Leica, Solms, Germany). Picrosirius red/Fast Green staining was quantified with Image-Pro Plus 5.1 (Media Cybernetics, Silver Spring, MD). The total area of each section was calculated as the area stained positive with

Picrosirius red plus the area stained positive with Fast Green. The relative collagen area was calculated as the area stained positive with Picrosirius red divided by the total area.

For determination of mast cell numbers, sections were incubated in 0.5% Toluidine Blue in 0.5 N HCl overnight, followed by 0.7 N HCl for 10 minutes. Eosin was used as a counterstain.

For immunohistochemistry, endogenous peroxidase was blocked with 1% H_2O_2 in methanol. Non-specific antibody binding was reduced by TBS containing 10% normal horse serum (Vector Laboratories, Burlingame, CA), 3% dry powdered milk and 0.2% BSA. Sections were incubated overnight at 4°C with mouse anti-CD2 (1:100, Cedarlane Laboratories, Burlington, NC) or mouse anti-CD68 (1:100, Abcam, Cambridge, MA), followed by horse anti-mouse IgG (1:400, Vector Laboratories), and an avidin-biotinperoxidase complex (Vector Laboratories). All immunostainings were visualized with 0.5 mg/mL 3,3-diaminobenzidine tetrahydrochloride (Sigma-Aldrich, St. Louis, MO) and 0.003% H_2O_2 in TBS. Hematoxylin was used as a counterstain.

Mitochondrial swelling assay

Rats were anesthetized with 3% isoflurane, the heart was isolated and about 200 mg of left ventricular tissue was minced and homogenized in 10 mL of a 10 mM HEPES buffer containing 225 mM mannitol, 75 mM sucrose and 0.1 mM EGTA, using a mechanical dounce homogenizer with a Teflon pestle. The homogenate was centrifuged at 700g for 10 minutes at 4°C. The supernatant was removed and centrifuged at 12,500g for 30 minutes to obtain the mitochondrial pellet. Pellets were resuspended in a 10 mM HEPES buffer containing 395 mM sucrose and 0.1 mM EGTA, washed twice, and immediately analyzed.

Mitochondrial permeability transition pore opening was measured by Ca^{2+} induced swelling, indicated by a decrease in absorbance at 540 nm. Isolated mitochondria were resuspended in swelling buffer containing 120 mM KCl, 10 mM Tris HCl, and 5 mM KH_2PO_4 to a final concentration of 150 μg/mL, and immediately exposed to vehicle, 250 μM $CaCl_2$, or 250 μM $CaCl_2$ in combination with 2 μM Cyclosporin A (CsA) as an inhibitor of transition pore opening. Optical density at 540 nm (OD540) was measured with a Synergy 4 microplate reader (BioTek, Winooski, VT), immediately before the assay and every 2 minutes thereafter for a total of 20 minutes.

RNA isolation and real-time PCR

Rats were anesthetized with 3% isoflurane, hearts were isolated and snap-frozen in liquid nitrogen. Frozen samples from the left ventricle were homogenized in Ultraspec™ RNA reagent (Biotecx Laboratories). After treatment with RQ-DNAse I (Promega, Madison, WI) at 37°C for 30 min, followed by DNAse inactivation at 75°C for 10 min, cDNA was synthesized using the High Capacity cDNA Archive Kit™ (Applied Biosystems). Steady-state mRNA levels were measured with real-time quantitative PCR (TaqMan™) using the 7500 Fast Real-Time PCR System and the following pre-designed assays for rat: B1 receptor (Rn02064589_s1), B2 receptor (Rn00597384_m1), NADPH oxidase (NOX)1 (Rn00586652_m1), NOX2 (Rn00576710_m1), NOX4 (Rn00585380_m1), and $p22^{phox}$ (CYBA, Rn00577357_m1) (all Applied Biosystems). Relative mRNA levels were calculated with the ΔΔCt method, using 18S rRNA as normalizer.

Western-Blots

Left ventricular tissue was homogenized in RIPA buffer with inhibitors of proteases (10 μL/mL) and phosphatases (10 μL/mL, Sigma Aldrich) and centrifuged at 20,000 g at 4°C for 15 minutes. Supernatant protein amounts were determined with a BCA assay (Sigma-Aldrich).

A total of 50 μg protein in Laemmli sample buffer containing β-mercaptoethanol (1:20 vol/vol) was boiled for 2-3 minutes, separated in Any kD™ Mini-Protean® polyacrylamide gels (Bio-Rad, Hercules, CA) at 100 Volts and transferred to PVDF membranes at 20 Volts overnight at 4°C.

Membranes were incubated in TBS containing 0.05% Tween-20 and 5% dry powdered milk, followed by rabbit antibodies against the following: phospho-Akt, phospho-Erk1/2, pan Akt, Erk1/2 (at 1:10,000), phospho-c-Jun (Ser63), phospho-c-Jun (Ser73), c-Jun (at 1:1,000), and HRP conjugated mouse anti-rabbit at 1:4,000 (for Akt and Erk1/2) or 1:10,000 (for c-Jun) (all Cell Signaling Technology, Danvers, MA). Protein loading was determined with mouse anti-GAPDH (1:20,000, Santa Cruz, Santa Cruz, CA), followed by HRP-conjugated goat anti-mouse (1:4,000, Jackson ImmunoResearch, West Grove, PA). Antibody binding was visualized with ECL™ Plus Detection reagent (GE Healthcare Life Sciences, Uppsala, Sweden) on CL-Xposure Film (Thermo Scientific, Waltham, MA). Films were scanned with an AlphaImager® gel documentation system (ProteinSimple, Santa Clara, CA) and bands were quantified with ImageJ.

Statistical analysis

Data were evaluated with the software package NCSS 2007 (NCSS, Kaysville, UT). Dose-dependencies were tested with linear regression. Data from Langendorff perfused heart preparations and mitochondrial swelling assays were tested with repeated measures ANOVA. All other data were analyzed with two-way ANOVA, followed by Newman-Keuls individual comparisons. The criterion for significance was a $p<0.05$. Data are reported as average ± standard error of the mean (SEM).

Results

This study investigated the role of the KKS in RIHD by comparing cardiac radiation injury in kininogen-deficient BN/Ka rats with injury in wild-type BN rats. *In vivo* cardiac function was measured with echocardiography at 3 months and 6 months after a single dose of 18 Gy or 24 Gy. All parameters and analyses of dose-dependencies are shown in Supplemental Tables S1-S6. Effects of radiation on M-mode parameters were more severe at 3 months after irradiation compared to 6 months (Supplemental Data S1). At 3 months, linear regression revealed a dose-dependent decrease in systolic LVID and volume in BN rats, together with a dose-dependent increase in systolic LVAW and LVPW thickness, EF and FS (Supplemental Data S2). On the other hand, stroke volume and cardiac output were not altered by irradiation. In BN/Ka rats, there was only a dose-dependent increase in systolic LVPW thickness, and borderline significance in EF and FS. In a direct comparison of the two genotypes, more severe changes were found in BN after 24 Gy in the following parameters: systolic LVID (Newman-Keuls: $p<0.02$) and volume ($p<0.04$), diastolic LVPW ($p<0.01$), EF ($p<0.05$), and FS ($p<0.04$).

In addition to M-mode analysis, strain analysis of the left ventricular endocardium in systole and diastole was performed (Supplemental Data S3-S6). Strain imaging, also known as deformation imaging, provides information about regional lengthening, shortening, and thickening of the myocardium. Strain is expressed as the percent change from the original size, while strain rate equals strain per unit of time. In accordance with an increase in EF and FS, at 3 months after irradiation both BN and BN/Ka rats showed dose-dependent increases in systolic radial velocity, displacement and strain, and circumferential velocity, strain, and strain rate (Supplemental Data S4). In diastole, both genotypes showed dose-dependent changes in radial velocity, circumferential velocity, and circumferential strain rate (Supplemental Data S6). In a direct comparison of the two genotypes, 24 Gy caused more severe changes in BN in the following parameters in systole: circumferential velocity

($p<0.03$), strain ($p<0.003$), strain rate ($p<0.003$), and radial velocity ($p<0.04$), displacement ($p<0.03$), and strain rate ($p<0.001$). In addition, BN rats showed larger changes in diastolic circumferential velocity ($p<0.03$), strain rate ($p<0.004$), and radial velocity ($p<0.03$).

In accordance with the echocardiography results at 6 months after irradiation, no significant effects of radiation on *ex vivo* cardiac Langendorff parameters were found in hearts isolated at this time point (data not shown). Heart to body weight ratios were not altered at 6 months after 18 Gy, but were significantly reduced from 3.0 ± 0.1 in sham-irradiated animals to 2.6 ± 0.1 and 2.7 ± 0.1 in BN and BN/Ka rats exposed to 24 Gy ($p<0.05$).

Since most severe cardiac function changes were seen at 3 months after a single dose of 24 Gy, left ventricular molecular changes were examined at this time point. Local heart irradiation caused a significant increase in gene expression of the kinin B2 receptor in both BN/Ka and BN rats (Table 1). B1 receptor transcripts could not be detected in sham-irradiated or in irradiated hearts (data not shown). Intracellular signaling upon kinin receptor activation involves Akt and Erk1/2. Local heart irradiation did not alter the left ventricular levels of total Erk1/2 or Akt. In addition, radiation-induced Akt phosphorylation was not statistically significant. On the other hand, a significant increase in phosphorylation of Erk1/2 and the Erk1/2 target c-Jun was observed in BN rats (Figure 1 and Supplemental Figures S7 and S8). No increased phosphorylation of Erk1/2 or c-Jun was found in BN/Ka rats.

Bradykinin may modify cardiac function and tissue remodeling by altering expression and activity of Nox enzyme complexes. We examined left ventricular mRNA levels of the main membrane components of the Nox complexes that are expressed in the heart: $p22^{phox}$, Nox1, Nox2, and Nox4. Nox 1 transcript levels were around the detection limit of the assay (data not shown), while $p22^{phox}$, Nox2, and Nox4 mRNAs could be detected in all samples. Local heart irradiation caused significant increases in Nox2 and Nox4 mRNA. No differences were found between BN/Ka rats and BN rats (Table 1).

Mitochondrial membrane integrity is important for cardiac function. Because bradykinin may alter the mitochondrial membrane, we investigated swelling in response to $CaCl_2$ in mitochondria isolated from BN and BN/Ka hearts. Enhanced swelling was observed in mitochondria isolated at 3 months after local heart irradiation, as shown by a reduction in their OD540 (Figure 2). The reduction in OD540 was inhibited with CsA, confirming that swelling was caused by enhanced mitochondrial transition pore opening. There was no difference between mitochondria isolated from irradiated BN hearts and mitochondria from irradiated BN/Ka hearts.

Histopathological changes at 6 months after irradiation included vacuolar degeneration of cardiomyocytes after 18 Gy and 24 Gy and local areas of severe cardiomyocyte degeneration and interstitial fibrosis after 24 Gy (Figure 3). Due to the local nature of the fibrosis, the total left ventricular area of interstitial collagen was not significantly altered by radiation exposure. In addition, no statistically significant differences were found between BN and BN/Ka rats (Figure 4).

The KKS modulates inflammation. We therefore determined the numbers of various inflammatory cells at 6 months after (sham)-irradiation (Figure 5). Radiation caused a dose-dependent reduction in the number of CD2-positive cells (T-cells and natural killer cells) in BN rats, but not in BN/Ka rats. In addition, radiation at a dose of 24 Gy caused a significant increase in the number of CD68-positive cells (monocytes and macrophages) in BN rats, but not in BN/Ka rats. Radiation at a dose of 24 Gy caused a significant increase in the number of mast cells in both genotypes.

Discussion

This study examined the role of the KKS in RIHD, by comparing the cardiac radiation response in kininogen-deficient BN/Ka rats with the response in wild-type BN rats. Local heart irradiation caused more severe changes in *in vivo* cardiac function and significantly altered the numbers of CD2-positive and CD68-positive cells in the wild-type BN rats only, suggesting a role for the KKS in cardiac function changes and recruitment of inflammatory cells in response to radiation. No obvious differences were found in myocardial degeneration and fibrosis, suggesting that the KKS may not play a significant role here.

BN and BN/Ka rats have been used to study the role of the kallikrein-kinin system in other cardiovascular diseases. BN/Ka rats are more prone to the induction of aortic aneurysms, but do not differ from BN rats in atherosclerosis (17). In myocardial infarct models, BN/Ka rats have shown to be more sensitive (27), or did not differ from BN rats (19), and showed a reduced response to angiotensin converting enzyme (ACE) inhibition (19). Hence, current and previous studies have shown that the KKS plays a distinct role in different models of cardiovascular disease. This may depend, in part, on B1 and B2 receptor expression and function.

Few studies have investigated the effects of radiation on cardiovascular bradykinin receptor expression and/or function. Whole body irradiation with a dose of 2 Gy enhanced immediate B1 receptor expression in the heart (28). *Ex vivo* beta and gamma irradiation of rabbit aorta induced B1 gene expression within hours after irradiation, and the response to B1 activation was enhanced (29). To our knowledge, this is the first study to examine left ventricular expression of bradykinin receptors several months after irradiation. We found an increase in left ventricular mRNA of the B2 receptor at 3 months after local heart irradiation, a time point at which in our rat model histopathological changes become apparent. The B2 receptor is constitutively expressed in the heart, while the B1 receptor is expressed only in certain conditions of inflammation or injury (9). While B2 expression was increased in both BN and BN/Ka rats, kinin signaling seemed to be impaired in BN/Ka rats, as shown by reduced phosphorylation of Erk1/2. Activation of Erk1/2 may have favorable effects in the heart, with its pro-survival and proangiogenic properties and promotion of cardiac contractility (30). Indeed, Erk1/2 activation is involved in beneficial cardiovascular effects of the KKS (31). Erk1/2 has a large array of target proteins, including many transcription factors. Together with c-Jun N-terminal kinase, Erk1/2 may activate c-Jun (30). As part of the activator protein-1 transcription complex, c-Jun may promote inflammation and the recruitment of macrophages (32). We found a radiation-induced increase in c-Jun phosphorylation in BN rats only, suggesting that this transcription factor may be part of the pathways by which the KKS regulates inflammation in the irradiated heart. To further determine mechanisms of action of the KKS, future studies may aim to identify protein phosphorylation patterns or transcription profiles induced by Erk1/2 in the wild-type BN rats.

In vivo analysis of cardiac function in this study included echocardiographic strain analysis, which is a method that gives direct measures of local contractility of the ventricular wall. This method is often considered more sensitive than conventional echocardiography. For instance, strain analysis shows early changes in those segments of the left ventricular wall that have been exposed to radiation during radiotherapy (33). It is also useful in the detection of local and global changes in the ventricular wall in small animal models (25). In our rat model, the increases in systolic strain, together with increases in EF and FS, but in the absence of a change in stroke volume, may reflect efforts of the irradiated hearts to maintain their cardiac output. Changes in echocardiography parameters were most severe at 3 months after irradiation with 24 Gy. While future studies will have to define the effects of

fractionated irradiation in BN and BN/Ka rats, here, we set out to determine potential mechanisms by which the KKS may affect cardiac function at 3 months after 24 Gy.

Studies have shown that bradykinin is able to both up-regulate and down-regulate expression and/or activity of Nox enzyme complexes (34, 35). The main function of Nox enzymes is the production of reactive oxygen species (ROS) by reducing oxygen to superoxide. The membrane-bound subunits of the Nox complexes consist of $p22^{phox}$ and $gp91^{phox}$. Of the known isoforms of $gp91^{phox}$, Nox1, Nox2 and Nox4 are expressed in the heart (36). Several studies have shown that ionizing radiation-induced upregulation of Nox expression may cause prolonged production of ROS, contributing to normal tissue radiation injury (37). Nox enzymes also play various roles in cardiac health and disease. Nox2 has been implicated in endothelial dysfunction (38) and adverse cardiac remodeling (39). Nox4, on the other hand, may have some cardioprotective properties, for instance by promoting neovascularization (40). We found an upregulation of both Nox2 and Nox4 gene expression after local heart irradiation in the rat, independent of genotype. The exact role of Nox complexes in RIHD remains to be determined.

Mitochondrial transition pore opening adversely affects cardiac function by causing ATP depletion, oxidative stress, dysregulation of Ca^{2+} homeostasis, and ultimately cardiac cell death (41). Local heart irradiation in this study caused enhanced mitochondrial transition pore activity, which may contribute to changes in cardiac function. The cause of mitochondrial transition pore activation after ionizing radiation is not known. Prolonged oxidative stress, as well as mitochondrial proteome changes may play a role (42, 43). Interestingly, bradykinin is known to alter the mitochondrial membrane and may prevent the opening of the mitochondrial transition pore (44). In this study, no differences were found between BN and BN/Ka after irradiation, suggesting that mitochondrial transition pore activity after the doses of radiation used in this study is not affected by the KKS.

The KKS is well known for its pro- and anti-inflammatory effects. Accordingly, BN and BN/Ka have different plasma profiles of certain inflammatory cytokines (17). Moreover, many inflammatory cells express kinin receptors (45) and may therefore be directly affected by the KKS. We examined cardiac numbers of inflammatory cells at 6 months after local heart irradiation in BN and BN/Ka rats. A dose-dependent reduction in the number of CD2-positive cells (T-cells and natural killer cells) was observed in BN rats, but not in BN/Ka rats. A single dose of 24 Gy caused an increase in the number of CD68-positive cells (monocytes and macrophages) in BN rats, but not in BN/Ka rats. These results show that the KKS affects the recruitment of various inflammatory cells. Inflammation plays a dual role in cardiac disease (46), and the exact role of the different subsets of inflammatory cells in RIHD needs to be determined.

Bradykinin can activate mast cells (47), and mast cell derived enzymes may interact with mediators of the KKS (8). In previous studies we found that cardiac mast cell numbers increase after local heart irradiation in the rat, coinciding with cardiac radiation injury, and mast cells may play a predominantly protective role in RIHD in the rat (26). In the current study, both histopathological changes and mast cell numbers were not altered by kininogen-deficiency. These results suggest that there is a close correlation between myocardial injury and mast cell numbers, but that the KKS may not be involved in mast cell recruitment. Whether the KKS modifies the function of cardiac mast cells after irradiation is still unknown.

This study suggests that pharmacological modification of the KKS may have beneficial effects on certain aspects of RIHD. Because of the dual role of the KKS in inflammation and cardioprotection, B1 and B2 receptor agonists and antagonists may each have positive and

negative effects on cardiac remodeling and function. For instance, ACE inhibitors are considered to be cardioprotective in part by their inhibition of bradykinin breakdown (48). While in experimental models of myocardial infarction a long-acting analog of bradykinin inhibited changes in cardiac function (49), a B2 receptor antagonist inhibited myocardial fibrosis (50). Studies are required to determine the effects of receptor agonists and antagonists in experimental models of RIHD.

In conclusion, this study shows that the KKS is involved in cardiac function changes and myocardial inflammatory infiltration in response to local irradiation. The KKS may have these effects at least in part by altering Erk1/2 signaling. Future studies have to address the effects of fractionated irradiation, as well as pharmacological modification of the KKS or its targets.

Supplementary Material

Refer to Web version on PubMed Central for supplementary material.

Acknowledgments

The authors acknowledge Dr. Sue A. Theus and Kimberly Henning for excellent support in animal care.

Financial support: National Institutes of Health (CA148679, M.B.; CA71382, M.H-J.) and the American Cancer Society (RSG-10-125-01-CCE, M.B.)

References

1. Adams MJ, Lipsitz SR, Colan SD, Tarbell NJ, Treves ST, Diller L, et al. Cardiovascular status in long-term survivors of Hodgkin's disease treated with chest radiotherapy. J Clin Oncol. 2004; 22:3139–48. [PubMed: 15284266]
2. Early Breast Cancer Trialists Collaborative Group. Favourable and unfavourable effects on long-term survival of radiotherapy for early breast cancer: an overview of the randomised trials. Lancet. 2000; 355:1757–70. [PubMed: 10832826]
3. Heidenreich PA, Kapoor JR. Radiation induced heart disease: systemic disorders in heart disease. Heart. 2009; 95:252–8. [PubMed: 19144884]
4. Chera BS, Rodriguez C, Morris CG, Louis D, Yeung D, Li Z, et al. Dosimetric comparison of three different involved nodal irradiation techniques for stage II Hodgkin's lymphoma patients: conventional radiotherapy, intensity-modulated radiotherapy, and three-dimensional proton radiotherapy. Int J Radiat Oncol Biol Phys. 2009; 75:1173–80. [PubMed: 19386423]
5. Kole TP, Aghayere O, Kwah J, Yorke ED, Goodman KA. Comparison of Heart and Coronary Artery Doses Associated with Intensity-Modulated Radiotherapy Versus Three-Dimensional Conformal Radiotherapy for Distal Esophageal Cancer. Int J Radiat Oncol Biol Phys. 2012 In press.
6. Wu WC, Chan CL, Wong YW, Cuijpers JP. A study on the influence of breathing phases in intensity-modulated radiotherapy of lung tumours using four-dimensional CT. Br J Radiol. 2009; 83:252–6. [PubMed: 19723769]
7. Imamura T, Dubin A, Moore W, Tanaka R, Travis J. Induction of vascular permeability enhancement by human tryptase: dependence on activation of prekallikrein and direct release of bradykinin from kininogens. Lab Invest. 1996; 74:861–70. [PubMed: 8642782]
8. Coffman LG, Brown JC, Johnson DA, Parthasarathy N, D'Agostino RB Jr. Lively MO, et al. Cleavage of high-molecular-weight kininogen by elastase and tryptase is inhibited by ferritin. Am J Physiol Lung Cell Mol Physiol. 2008; 294:L505–L515. [PubMed: 18192590]
9. Manolis AJ, Marketou ME, Gavras I, Gavras H. Cardioprotective properties of bradykinin: role of the B(2) receptor. Hypertens Res. 2010; 33:772–7. [PubMed: 20505673]
10. Spillmann F, Altmann C, Scheeler M, Barbosa M, Westermann D, Schultheiss HP, et al. Regulation of cardiac bradykinin B1- and B2-receptor mRNA in experimental ischemic, diabetic,

and pressure-overload-induced cardiomyopathy. Int Immunopharmacol. 2002; 2:1823–32. [PubMed: 12489796]

11. Agata J, Chao L, Chao J. Kallikrein gene delivery improves cardiac reserve and attenuates remodeling after myocardial infarction. Hypertension. 2002; 40:653–9. [PubMed: 12411458]
12. Sun D, Shen M, Li J, Li W, Zhang Y, Zhao L, et al. Cardioprotective effects of tanshinone IIA pretreatment via kinin B2 receptor-Akt-GSK-3beta dependent pathway in experimental diabetic cardiomyopathy. Cardiovasc Diabetol. 2011; 10:4. [PubMed: 21232147]
13. Koike MK, de Carvalho FC, de Lourdes HM. Bradykinin B2 receptor antagonism attenuates inflammation, mast cell infiltration and fibrosis in remote myocardium after infarction in rats. Clin Exp Pharmacol Physiol. 2005; 32:1131–6. [PubMed: 16445581]
14. Kim NN, Villegas S, Summerour SR, Villarreal FJ. Regulation of cardiac fibroblast extracellular matrix production by bradykinin and nitric oxide. J Mol Cell Cardiol. 1999; 31:457–66. [PubMed: 10093057]
15. Yin H, Chao L, Chao J. Nitric oxide mediates cardiac protection of tissue kallikrein by reducing inflammation and ventricular remodeling after myocardial ischemia/reperfusion. Life Sci. 2008; 82:156–65. [PubMed: 18068196]
16. Damas J. The brown Norway rats and the kinin system. Peptides. 1996; 17:859–72. [PubMed: 8844778]
17. Kaschina E, Stoll M, Sommerfeld M, Steckelings UM, Kreutz R, Unger T. Genetic kininogen deficiency contributes to aortic aneurysm formation but not to atherosclerosis. Physiol Genomics. 2004; 19:41–9. [PubMed: 15238617]
18. Koch M, Bonaventura K, Spillmann F, Dendorfer A, Schultheiss HP, Tschope C. Attenuation of left ventricular dysfunction by an ACE inhibitor after myocardial infarction in a kininogen-deficient rat model. Biol Chem. 2008; 389:719–23. [PubMed: 18627293]
19. Liu YH, Yang XP, Mehta D, Bulagannawar M, Scicli GM, Carretero OA. Role of kinins in chronic heart failure and in the therapeutic effect of ACE inhibitors in kininogen-deficient rats. Am J Physiol Heart Circ Physiol. 2000; 278:H507–H514. [PubMed: 10666082]
20. Van Luijk P, Faber H, Meertens H, Schippers JM, Langendijk JA, Brandenburg S, et al. The impact of heart irradiation on dose-volume effects in the rat lung. Int J Radiat Oncol Biol Phys. 2007; 69:552–9. [PubMed: 17869668]
21. Huang EX, Hope AJ, Lindsay PE, Trovo M, El N,I, Deasy JO, et al. Heart irradiation as a risk factor for radiation pneumonitis. Acta Oncol. 2011; 50:51–60. [PubMed: 20874426]
22. Hayashi I, Oh-ishi S. Plasma kininogen deficiency: associated defective secretion of kininogens by primary cultures of hepatocytes from brown Norway Katholiek rats. J Biochem. 1993; 113:531–7. [PubMed: 8340346]
23. Damas J, Adam A. Congenital deficiency in plasma kallikrein and kininogens in the brown Norway rat. Experientia. 1980; 36:586–7. [PubMed: 6900563]
24. Devic S, Seuntjens J, Sham E, Podgorsak EB, Schmidtlein CR, Kirov AS, et al. Precise radiochromic film dosimetry using a flat-bed document scanner. Med Phys. 2005; 32:2245–53. [PubMed: 16121579]
25. Bauer M, Cheng S, Jain M, Ngoy S, Theodoropoulos C, Trujillo A, et al. Echocardiographic speckle-tracking based strain imaging for rapid cardiovascular phenotyping in mice. Circ Res. 2011; 108:908–16. [PubMed: 21372284]
26. Boerma M, Wang J, Wondergem J, Joseph J, Qiu X, Kennedy RH, et al. Influence of mast cells on structural and functional manifestations of radiation-induced heart disease. Cancer Res. 2005; 65:3100–7. [PubMed: 15833839]
27. Ito H, Hayashi I, Izumi T, Majima M. Bradykinin inhibits development of myocardial infarction through B2 receptor signalling by increment of regional blood flow around the ischaemic lesions in rats. Br J Pharmacol. 2003; 138:225–33. [PubMed: 12522094]
28. Shukla J, Khan NM, Thakur VS, Poduval TB. L-arginine mitigates radiation-induced early changes in cardiac dysfunction: the role of inflammatory pathways. Radiat Res. 2011; 176:158–69. [PubMed: 21663395]

29. Levesque L, Lam MH, Allaire P, Mondat M, Houle S, Beaudoin G, et al. Effects of radiation therapy on vascular responsiveness. J Cardiovasc Pharmacol. 2001; 37:381–93. [PubMed: 11300651]
30. Rose BA, Force T, Wang Y. Mitogen-activated protein kinase signaling in the heart: angels versus demons in a heart-breaking tale. Physiol Rev. 2010; 90:1507–46. [PubMed: 20959622]
31. Yan JT, Wang T, Wang DW. Recombinant adeno-associated virus-mediated human kallikrein gene therapy protects against hypertensive target organ injuries through inhibiting cell apoptosis. Acta Pharmacol Sin. 2009; 30:1253–61. [PubMed: 19684610]
32. Feinberg MW, Shimizu K, Lebedeva M, Haspel R, Takayama K, Chen Z, et al. Essential role for smad3 in regulating MCP-1 expression and vascular inflammation. Circ Res. 2004; 94:601–8. [PubMed: 14752027]
33. Erven K, Jurcut R, Weltens C, Giusca S, Ector J, Wildiers H, et al. Acute radiation effects on cardiac function detected by strain rate imaging in breast cancer patients. Int J Radiat Oncol Biol Phys. 2011; 79:1444–51. [PubMed: 20605341]
34. Woodfin A, Hu DE, Sarker M, Kurokawa T, Fraser P. Acute NADPH oxidase activation potentiates cerebrovascular permeability response to bradykinin in ischemia-reperfusion. Free Radic Biol Med. 2011; 50:518–24. [PubMed: 21167936]
35. Dias JP, Talbot S, Senecal J, Carayon P, Couture R. Kinin B1 receptor enhances the oxidative stress in a rat model of insulin resistance: outcome in hypertension, allodynia and metabolic complications. PLoS One. 2010; 5:e12622. [PubMed: 20830306]
36. Nabeebaccus A, Zhang M, Shah AM. NADPH oxidases and cardiac remodelling. Heart Fail Rev. 2011; 16:5–12. [PubMed: 20658317]
37. Wang Y, Liu L, Pazhanisamy SK, Li H, Meng A, Zhou D. Total body irradiation causes residual bone marrow injury by induction of persistent oxidative stress in murine hematopoietic stem cells. Free Radic Biol Med. 2010; 48:348–56. [PubMed: 19925862]
38. Zhang P, Hou M, Li Y, Xu X, Barsoum M, Chen Y, et al. NADPH oxidase contributes to coronary endothelial dysfunction in the failing heart. Am J Physiol Heart Circ Physiol. 2009; 296:H840–H846. [PubMed: 19168727]
39. Zhao Y, McLaughlin D, Robinson E, Harvey AP, Hookham MB, Shah AM, et al. Nox2 NADPH oxidase promotes pathologic cardiac remodeling associated with Doxorubicin chemotherapy. Cancer Res. 2010; 70:9287–97. [PubMed: 20884632]
40. Craige SM, Chen K, Pei Y, Li C, Huang X, Chen C, et al. NADPH oxidase 4 promotes endothelial angiogenesis through endothelial nitric oxide synthase activation. Circulation. 2011; 124:731–40. [PubMed: 21788590]
41. Di Lisa F, Carpi A, Giorgio V, Bernardi P. The mitochondrial permeability transition pore and cyclophilin D in cardioprotection. Biochim Biophys Acta. 2011; 1813:1316–22. [PubMed: 21295622]
42. Barjaktarovic Z, Schmaltz D, Shyla A, Azimzadeh O, Schulz S, Haagen J, et al. Radiation-induced signaling results in mitochondrial impairment in mouse heart at 4 weeks after exposure to x-rays. PLoS One. 2011; 6:e27811. [PubMed: 22174747]
43. Imaizumi N, Aniya Y. The role of a membrane-bound glutathione transferase in the peroxynitrite-induced mitochondrial permeability transition pore: formation of a disulfide-linked protein complex. Arch Biochem Biophys. 2011; 516:160–72. [PubMed: 22050912]
44. Park SS, Zhao H, Mueller RA, Xu Z. Bradykinin prevents reperfusion injury by targeting mitochondrial permeability transition pore through glycogen synthase kinase 3beta. J Mol Cell Cardiol. 2006; 40:708–16. [PubMed: 16516918]
45. Bockmann S, Paegelow I. Kinins and kinin receptors: importance for the activation of leukocytes. J Leukoc Biol. 2000; 68:587–92. [PubMed: 11073095]
46. Jiang B, Liao R. The paradoxical role of inflammation in cardiac repair and regeneration. J Cardiovasc Transl Res. 2010; 3:410–6. [PubMed: 20559773]
47. Wei CC, Hase N, Inoue Y, Bradley EW, Yahiro E, Li M, et al. Mast cell chymase limits the cardiac efficacy of Ang I-converting enzyme inhibitor therapy in rodents. J Clin Invest. 2010; 120:1229–39. [PubMed: 20335663]

48. Fleming I. Signaling by the angiotensin-converting enzyme. Circ Res. 2006; 98:887–96. [PubMed: 16614314]

49. Marketou M, Kintsurashvili E, Papanicolaou KN, Lucero HA, Gavras I, Gavras H. Cardioprotective effects of a selective B(2) receptor agonist of bradykinin post-acute myocardial infarct. Am J Hypertens. 2010; 23:562–8. [PubMed: 20186129]

50. Koike MK, de Carvalho FC, de Lourdes HM. Bradykinin B2 receptor antagonism attenuates inflammation, mast cell infiltration and fibrosis in remote myocardium after infarction in rats. Clin Exp Pharmacol Physiol. 2005; 32:1131–6. [PubMed: 16445581]

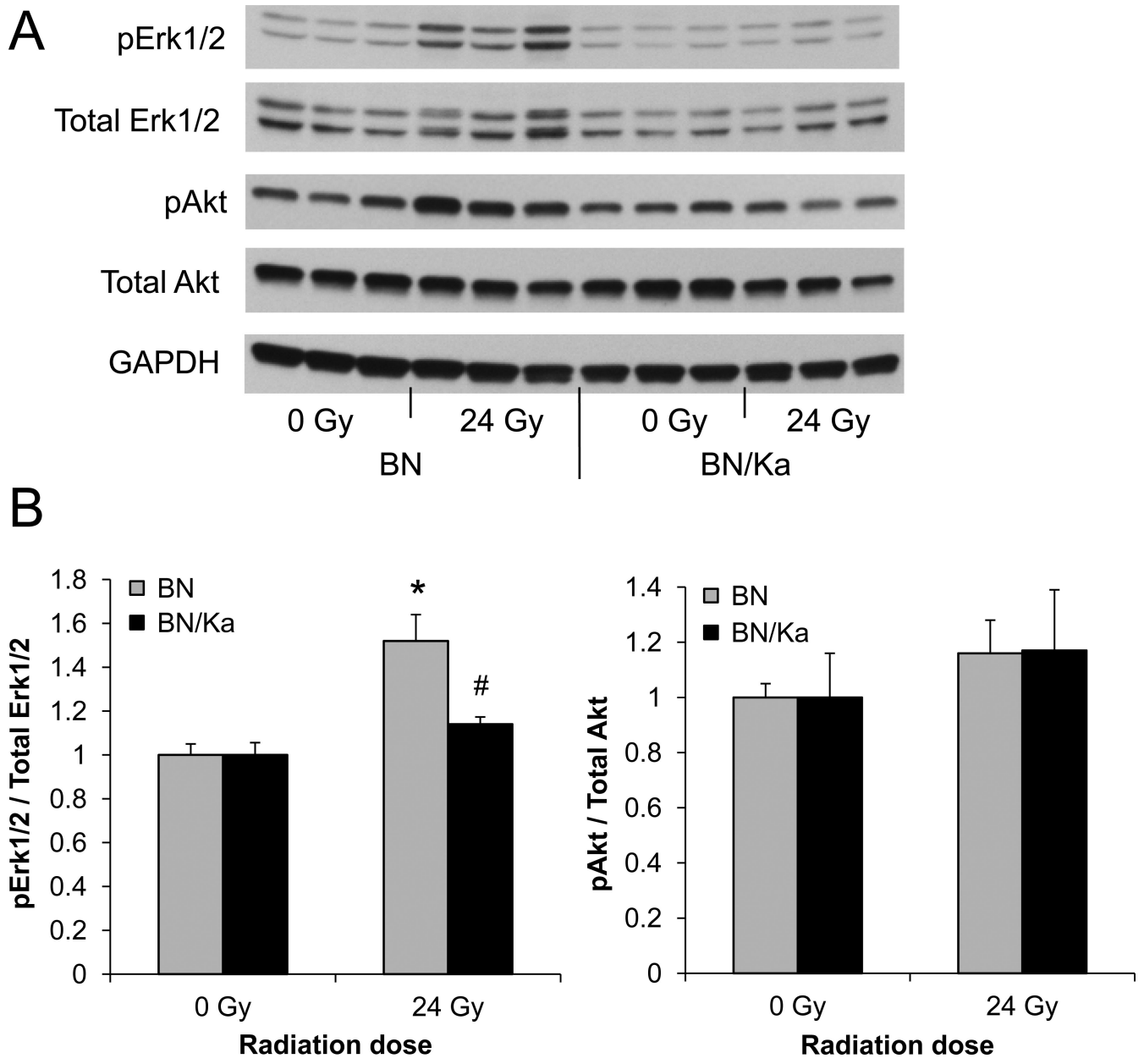

Figure 1.

Western-Blot analysis of Akt and Erk1/2 at 3 months after sham-irradiation or 24 Gy. A) Representative cropped image of total and phosphorylated Akt and Erk1/2 in BN and BN/Ka rats. Full-length blots are shown in Supplementary Data S7. B) Quantification of phosphorylated Akt or Erk1/2 divided by total Akt or Erk1/2, relative to sham-irradiated samples. Average ± SEM, n=6 (*Significant difference with 0 Gy, $^{\#}$Significant difference between BN and BN/Ka, $p<0.01$).

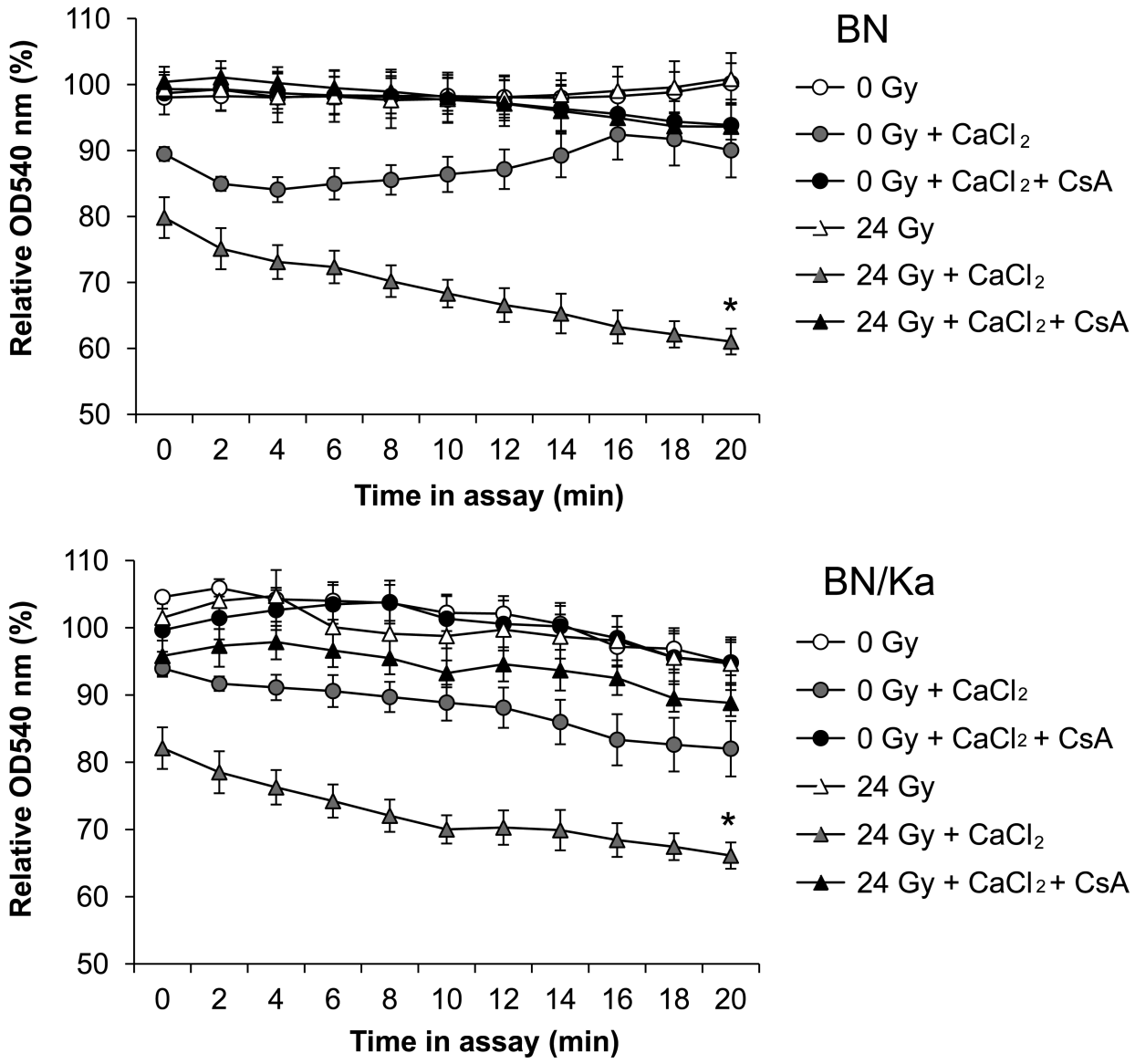

Figure 2.

Mitochondrial swelling assay at 3 months after local heart irradiation. For each curve, the optical density at 540 nm was calculated relative to the optical density of the isolated mitochondria immediately before the assay. CsA was added as an inhibitor of mitochondrial transition pore opening. For clarity, the SEM of only two datasets in each graph is shown (n=6, *Significant difference between 0 Gy + $CaCl_2$ and 21 Gy + $CaCl_2$, $p<0.005$ as shown with repeated measures ANOVA (Response variable = relative OD540; Between factor = experimental group; Within factor = time in assay)).

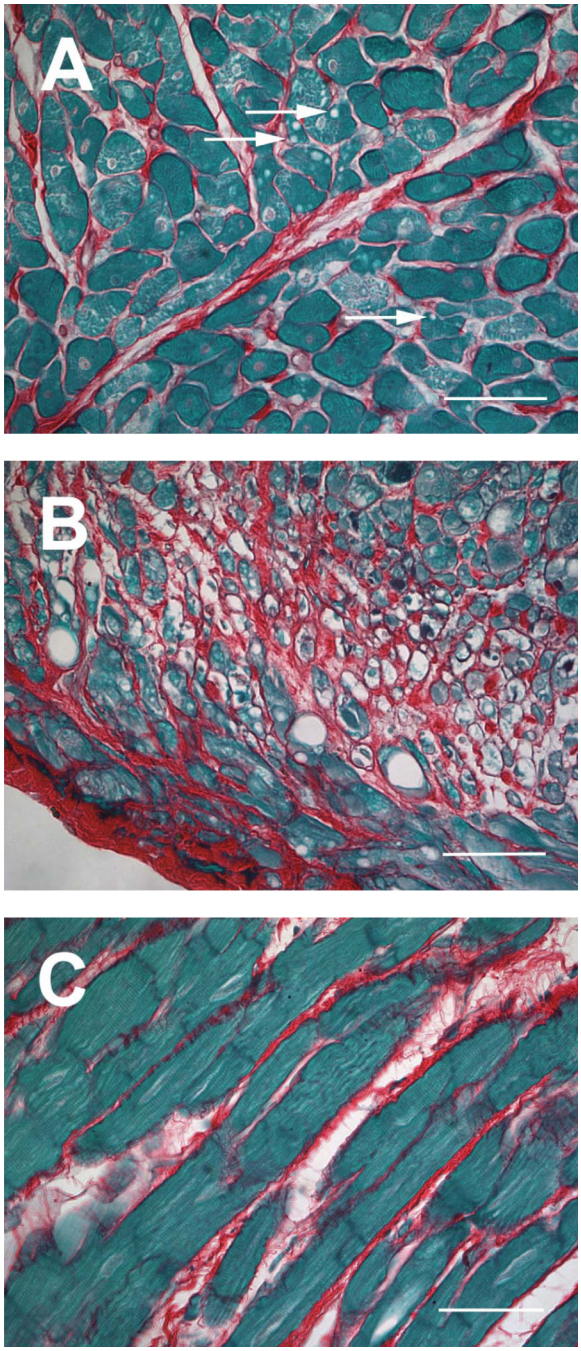

Figure 3.
Histopathological changes at 6 months after local heart irradiation. A) Vacuolar degeneration of cardiomyocytes after 18 Gy (arrows); B) Severe cardiomyocyte degeneration after 24 Gy; C) Interstitial fibrosis after 24 Gy. Sirius Red and Fast Green staining, 40x objective (scale bar: 50 μm).

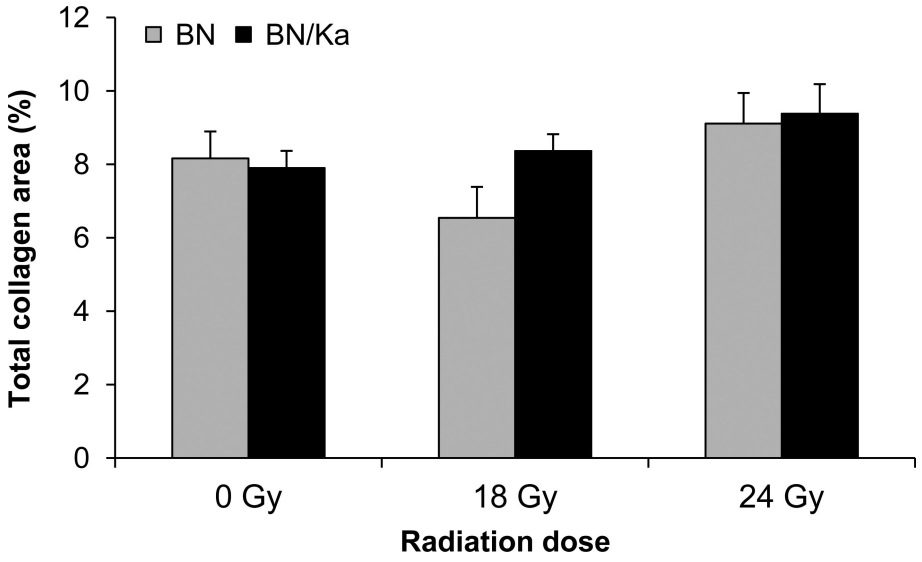

Figure 4.

Total interstitial collagen area as measured with computerized image analysis of Sirius Red / Fast Green stained sections at 6 months after local heart irradiation. Average ± SEM, n=6-9. There were no statistically significant differences between the two genotypes or between radiation groups.

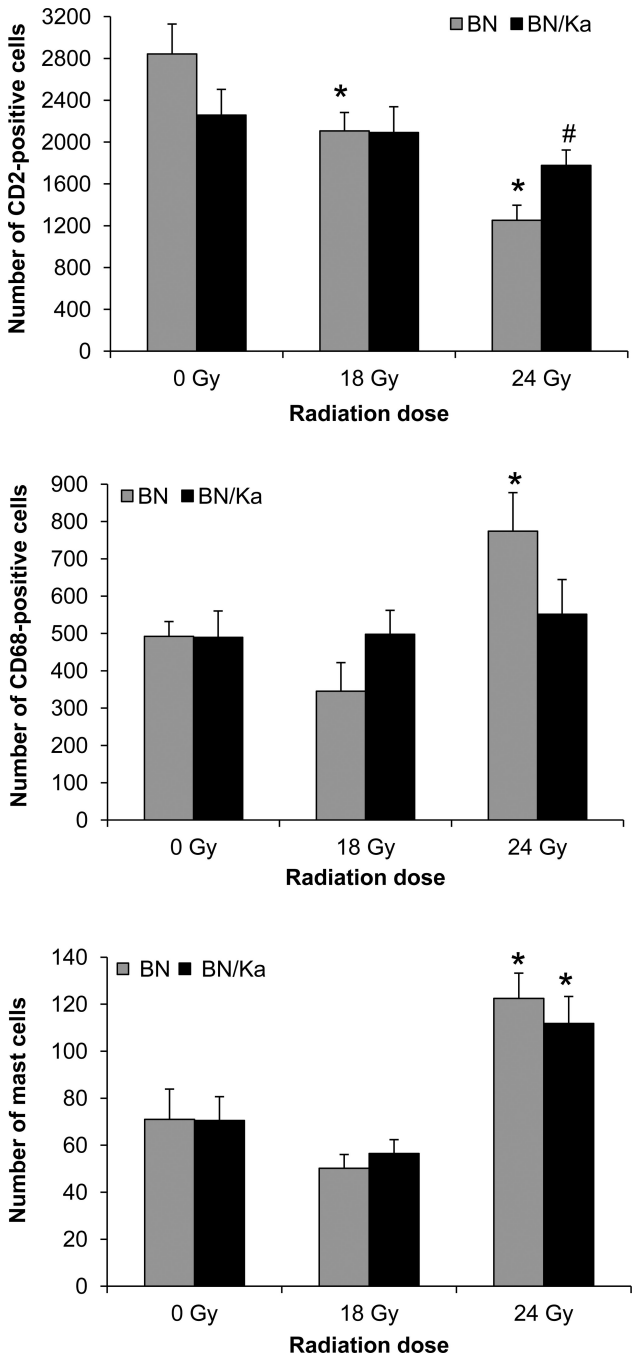

Figure 5.

Numbers of CD2-positive cells, CD68-positive cells, and mast cells in the heart at 6 months after irradiation. Average ± SEM, n=6-9 (*Significant difference with 0 Gy, #Significant difference between BN and BN/Ka, $p<0.05$).

Table 1

Left ventricular mRNA values of the B2 receptor and of membrane components of Nox complexes at 3 months after 24 Gy or 0 Gy, relative to BN after 0 Gy (average ± SEM, n=6).

	BN		BN/Ka	
	0 Gy	**24 Gy**	**0 Gy**	**24 Gy**
B2 receptor	1.11 ± 0.22	2.24 ± 0.37 *	0.99 ± 0.24	2.26 ± 0.61 *
Nox2	1.03 ± 0.10	1.50 ± 0.22 *	0.99 ± 0.07	1.64 ± 0.25 *
Nox4	1.06 ± 0.19	2.34 ± 0.43 *	1.54 ± 0.39	2.36 ± 0.60 *
$p22^{phox}$	1.01 ± 0.07	1.15 ± 0.09	1.17 ± 0.05	1.20 ± 0.08

* Significant difference with 0 Gy ($p<0.05$)